REPORT DOCUMENTATION PAGE

Form Approved
OMB No. 0704-0188

Public reporting burden for this collection of information is estimated to average 1 hour per response, including the time for reviewing instructions, searching existing data sources, gathering and maintaining the data needed, and completing and reviewing this collection of information. Send comments regarding this burden estimate or any other aspect of this collection of information, including suggestions for reducing this burden to Department of Defense, Washington Headquarters Services, Directorate for Information Operations and Reports (0704-0188), 1215 Jefferson Davis Highway, Suite 1204, Arlington, VA 22202-4302. Respondents should be aware that notwithstanding any other provision of law, no person shall be subject to any penalty for failing to comply with a collection of information if it does not display a currently valid OMB control number. **PLEASE DO NOT RETURN YOUR FORM TO THE ABOVE ADDRESS.**

1. REPORT DATE *(DD-MM-YYYY)*	2. REPORT TYPE	3. DATES COVERED *(From - To)*
11/12/02	FINAL TECHNICAL REPORT	01/01/97 – 06/30/02

4. TITLE AND SUBTITLE
Lateral and Vertical Mixing in Marginal Seas (2001-2002).
Topographic Influence on Small-Scale Ocean Dynamics (1999-2000).
Mixing, Fine-Structure, and Internal Waves near Shallow-Summit Seamounts (1997-1998).

5a. CONTRACT NUMBER

5b. GRANT NUMBER
N00014-97-1-0140

5c. PROGRAM ELEMENT NUMBER

6. AUTHOR(S)
Dr. Iossif Lozovatsky
Dr. Harindra Fernando

5d. PROJECT NUMBER

5e. TASK NUMBER

5f. WORK UNIT NUMBER

7. PERFORMING ORGANIZATION NAME(S) AND ADDRESS(ES)

Arizona State University
Dept. of Mechanical and
Aerospace Engineering
Tempe, AZ 85287-6106

8. PERFORMING ORGANIZATION REPORT NUMBER

XAA 0027/TE

9. SPONSORING / MONITORING AGENCY NAME(S) AND ADDRESS(ES)
Office of Naval Research   Dr. Steven Murray
Ballston Centre Tower One
800 North Quincy Street
Arlington, VA 22217-5660

10. SPONSOR/MONITOR'S ACRONYM(S)
ONR

11. SPONSOR/MONITOR'S REPORT NUMBER(S)

12. DISTRIBUTION / AVAILABILITY STATEMENT

Approved for Public Release; distribution is Unlimited.

13. SUPPLEMENTARY NOTES

20021126 046

14. ABSTRACT
Small, fine, and meso-scale structures in deep and littoral oceans were studied using field observations, data analysis and numerical simulations. The archives of data collected by Russian oceanographers were scrutinized for data quality and posted on the web for the use of international community. Three new trans-Atlantic cruises focusing on marginal zones were organized in collaboration with Russian and Spanish scientists. The influence of topography on oceanic flows was investigated on shelves and continental slopes, around seamounts and near submarine ridges. The excessive energy of internal tides produces enhanced mixing in the pycnocline at a distance up to 1000 km from the topography. The extensive turbulent "columns" were discovered above the seamount summits; the diffusivities exceed the background values by two orders of magnitude. Study of shelf mixing turbulence and internal waves in semi-enclosed basins showed that short internal waves generated at the tidal shelf break of the Peter the Great Bay can produce vertical diffusivities in the pycnocline up to 10^{-3} m^2/s, which is about an order of magnitude higher than on the Black Sea non-tidal shelf. Numerical modeling was focused on the formation of step-like structure in the thermocline due to boundary forcing. A new parameterization for the patch turbulence was suggested using the normalized Thorpe scale.

15. SUBJECT TERMS
Mixing, turbulence, fine structure, internal waves, tides, shelves, seamounts, semi-enclosed seas

16. SECURITY CLASSIFICATION OF:			17. LIMITATION OF ABSTRACT	18. NUMBER OF PAGES	19a. NAME OF RESPONSIBLE PERSON Iossif Lozovatsky
a. REPORT	b. ABSTRACT	c. THIS PAGE		25	19b. TELEPHONE NUMBER *(include area code)* (480) 965-5597

Standard Form 298 (Rev. 8-98)
Prescribed by ANSI Std. Z39.18

Lateral and Vertical Mixing in Marginal Seas (2001-2002)

Topographic Influence on Small-Scale Oceanic Dynamics (1999-2000)

Mixing, Fine-Structure and Internal Waves near Shallow-Summit Seamounts (1997-1998)

I. D. Lozovatsky

Environmental Fluid Dynamics Program, Department of Mechanical & Aerospace Engineering
Arizona State University, Tempe, AZ 85287-9809
phone: 480-965-5597, fax: 480-965-8746, e-mail: i.lozovatsky@asu.edu

H. J. S. Fernando

Environmental Fluid Dynamics Program, Department of Mechanical & Aerospace Engineering,
Arizona State University, Tempe, AZ 85287-9809,
phone: 480-965-2807, fax: 480-965-8746, e-mail: J.Fernando@asu.edu

FINAL REPORT

LONG TERM GOALS

The long-term goals of our research are to identify and evaluate key processes responsible for the generation, maintenance, and decay of vertical and lateral mixing that influences transports of heat, energy, momentum, dissolved matter and plankton in the ocean. Turbulent mixing induced in boundary layers and marginal zones in deep and littoral oceans is the current thrust of our work. Intermittent turbulence in coastal and deep regions and associated background mesoscale dynamics are studied by comprehensive analyses of special field measurements as well as using theoretical and numerical modeling.

OBJECTIVES

The prime objective of the work reported herein was to acquire a better understanding of the oceanic fine structure generated by turbulent mixing and internal-wave dynamics in regions of abrupt topography of coastal and deep oceans. This study is important, in particular, for modeling and calculation of vertical transports through the highly stratified seasonal pycnocline

in mid-latitudes. Evaluation of the influence of boundary mixing on the basin-averaged turbulent diffusivity is also of interest so as the development of parameterizations for turbulent mixing in rotating, stratified shear flows that can be used to formulate a model for thermohaline fine-structure formation in the pycnocline due to forcing at oceanic boundaries.

During the course of the research, we focused on studying the decay of turbulence downstream of seamounts and analyzing statistics of topography-induced mixing in different oceanic layers. The decay of tidal internal-wave energy downstream of submarine ridges in deep ocean and internal-wave induced fluxes in the coastal zone was also considered.

Another aspect of our study was the influence of vertical shear on the nature of turbulence on shallow shelves. The impact of background shear on the generation of density fine structure induced by boundary forcing appears to be an important phenomenon that should be considered in parameterization of ocean mixing processes, and to this end we embarked on a study that delved into this aspect using numerical modeling.

An important part of the project was the development of a web-accessible an extensive database of mooring and profiling measurements taken by Russian oceanographers in deep basins of the Atlantic, Pacific, and Indian oceans and in the marginal seas of the western Pacific. This effort was aimed at preserving a significant portion of unique oceanographic data obtained by oceanographers from the Former Soviet Union during two decades of extensive field campaigns and to make them available for the western scientific community.

Collecting of new oceanographic data on mesoscale ocean dynamics was also an important concern of our work. Organizing new field campaigns in cooperation with Russian, Spanish, and Canadian scientists was intended to conduct hydrographic and turbulent measurements at several transects across the Atlantic and collect new basin-scale data to be used for research.

The project results described below include field measurements, processing of observational data as well as numerical and theoretical analyses. The dissemination of information was achieved through pier reviewed international journals, development of a web accessible database and via maintaining a web page http://ceaspub.eas.asu.edu/oceanrus .

SCIENTIFIC RESULTS

B. The Decay of Turbulence Downstream of Seamounts

The kinetic energy dissipation rate and turbulent diffusivities obtained along sixty-miles NW - SE transect, centered at the summit of seamount Irving (subtropical eastern Atlantic), revealed an enormous enhancement of turbulent mixing above the summit (the depth of which is 260 m) of the seamount (Fig. A1, left panel).
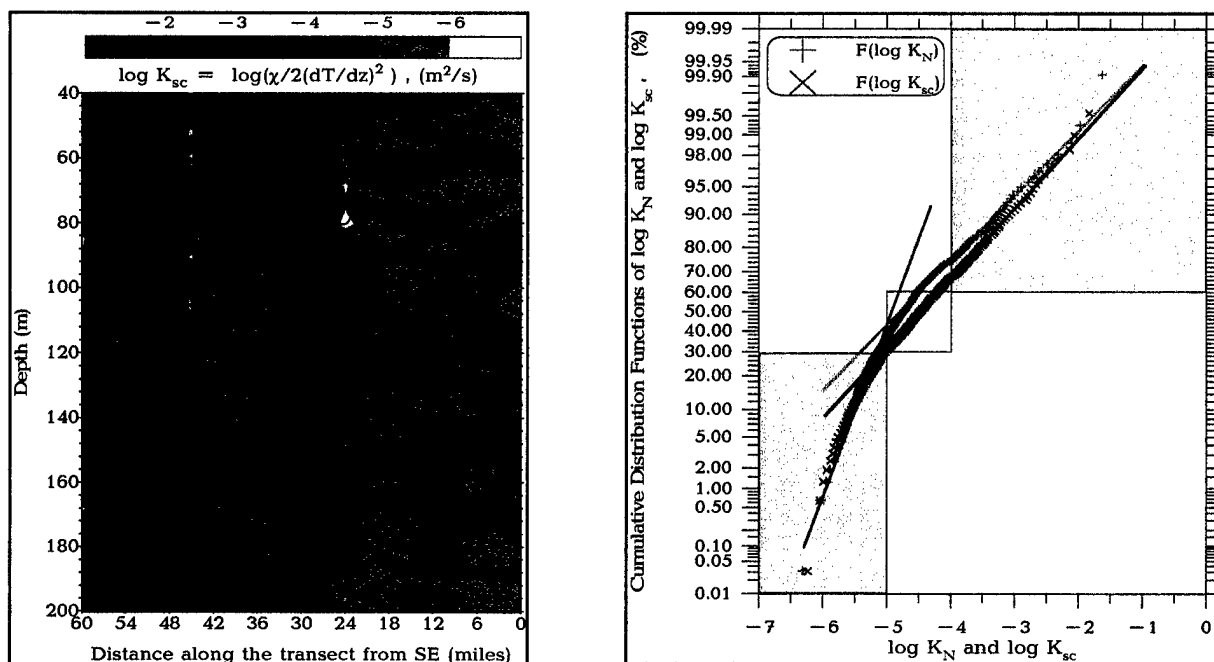

Fig. A1. *Left Panel*: A cross-section of the scalar diffusivity. The top of seamount Irving (z = 260 m) is in the middle of the section (a black triangle). *Right Panel*: Cumulative probability distributions of turbulent diffusivities along the transect in the depth range 40 - 200 m (below the upper thermohalocline). The straight lines show possible log-normal fits for the upper ($K > 10^{-5}$ m^2/s) and lower ($K < 10^{-5}$ m^2/s) portions of the distributions.

A "turbulent column" more than two hundred meters of height was generated in a vicinity of the local frontal zone associated with an anticyclonic topographic eddy (the slope of isopycnal surfaces of the eddy exceeded 0.005). A turbulent region of approximately the same height was also found above the Fieberling Guyot [*Kunze and Tool*, 1997]. Such powerful mixing events, with the mean kinetic energy dissipation rate of $\bar{\varepsilon} = (6 \pm 1) \times 10^{-8}$ W/kg in our case, may significantly elevate the turbulent diffusivity in the area. The cumulative distribution functions of mass K_N and scalar K_{sc} diffusivities (Fig. A1, right panel), calculated for the depth range of

40-200 m along the transect, ensured that the bootstrap estimates of the mean are in the range of $(3.8-5.1)\times10^{-4}$ m²/s with 90% confidence limits of $(3.1-6.1)\times10^{-4}$ m²/s. This implies that the averaged mixing rate in a 60-mile diameter and 150 m high region surrounding the seamount is 30-60 times than that of the far field value. At the place of generation, the diffusivities, averaged over the stratified water column were as high as $(1-2)\times10^{-3}$ m²/s; a similar result was reported by *Kunze and Tool* [1997]. Turbulent "columns" above seamounts seem to be skewed toward the rim area. Our observations at seamount Irving and those of *Kunze and Tool* [1997] at Fieberling seamount showed that the turbulent "columns" are possibly detached from the bottom. Their origin appears to be related to the internal-wave shear, rather than to the bottom-roughness induced turbulence.

More regular, frictional boundary layers occupy about 30% of the water column above the summit of the Ampere seamount (Fig. A2). The dissipation rate within these stratified, non-fully mixed layers was high, $(1-9)\times10^{-7}$ W/kg, and corresponding scalar diffusivities ranged $(5-70)\times10^{-4}$ m²/s.

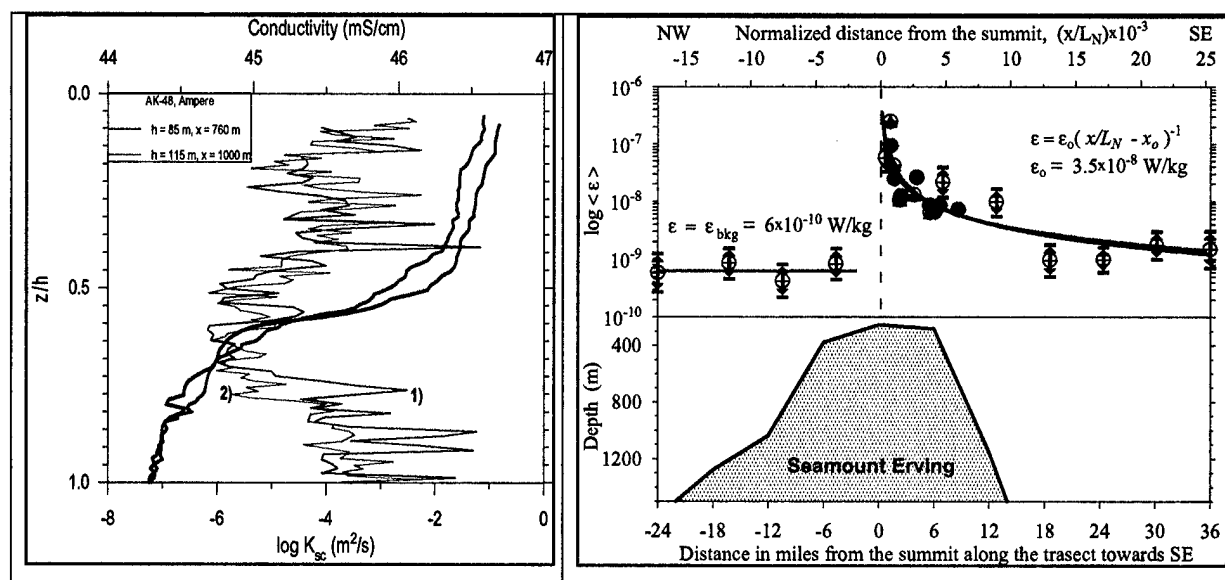Fig. A2. *Left Panel*: Scalar diffusivities and mean conductivity profiles near the rim of Ampere seamount plotted as a function of the normalized depth z/h, h - the depth of the seamount floor. *Right Panel*: The averaged dissipation rate at the Irving transect (circles) and downstream of the Ampere seamount (triangles) and Howland Island (diamonds). An inverse-power trend is fitted for the decrease of $\varepsilon(x/L_N)$.

The variation of $\bar{\varepsilon}$ along the Irving transect is shown in Fig. A2, right panel. The results correspond the depth range 90-140 m, which has a weak and relatively undisturbed mean stratification. It is clear, that turbulence upstream of the seamount is almost unaffected by the topography, showing a low background level of 6×10^{-10} W/kg. However, the dissipation decreases from 6×10^{-8} to about $(1-2)\times10^{-9}$ W/kg downstream of the summit over a distance of 36 miles. This trend was approximated by a power laws $\bar{\varepsilon} = \bar{\varepsilon}_o (\tilde{x} - \tilde{x}_o)^{-n}$, in parallel with the methodology used for laboratory grid-generated turbulence; $\bar{\varepsilon}_o$ is the dissipation rate at the normalized location $\tilde{x}_o$ of the topography-induced mixing (summit, rim or flank), $\tilde{x} = x/\bar{L}$ and the Ozmidov scale $\bar{L}$ is based on $\bar{\varepsilon}_o$. Note that the grid turbulence in stratified tunnels shows $\varepsilon(x)$ dependence close to x^{-2}. The least-square fitting applied for the Irving data (circles) gives n = 1 and $\bar{\varepsilon}_o = 3.5\times10^{-8}$ W/kg. The data taken from other regions, e.g. turbulent wakes downstream of the Ampere seamount (triangles) and Howland Island (diamonds), also follow the power law trend x^{-1}, showing the versatility of the results obtained. This suggests that vertical shear induced by internal waves and topographic eddies supports turbulence far from the turbulence source. The decay of $\bar{\varepsilon}$ according to $\bar{\varepsilon} \sim \tilde{x}^{-1}$ is typically superimposed with smaller scale fluctuations induced by inhomogeneities. It appears that, turbulence first decays rapidly over distances of the order of a few hundreds meters from the source, then grows owing to the interaction with strong shear and finally decays more gradually. This preliminary scenario must be further verified by future research.

The ratio between turbulent buoyancy flux and kinetic energy dissipation rate, known as the mixing efficiency γ, is significantly affected by topographically induced turbulence. We found $\gamma < 0.2$ for almost all depths above the seamount Irving. Since the activity parameter, $A_G \sim \gamma^{-1/2}$, exceeded 0.6 while the buoyancy Reynolds number $Re_b \equiv \varepsilon/30\nu N^2$ exceeded 1, the turbulence in the upper 200 meter layer appears to be active based on *Gibson's* fossil turbulent theory [1980]. However, the least-squared fit to A_G - Re_b data indicated $A_G = 0.2\times Re_b^{1/3}$, which deviates from Gibson prediction, $A_G \sim Re_b^{1/2}$. This shows that some other governing parameters are significant for mixing activities close to solid boundaries. The approximation obtained for $\hat{Re}_b(\hat{Ri})$ leads to the following expression for ratio of buoyancy K_b

and momentum K_M diffusivities, $K_b/K_M = Ri^{-1}$, if a stationary balance of the turbulent kinetic energy is in existence. The later formula is in general agreement with the parameterizations used for the turbulent Prandtl number K_M/K_b in our numerical modeling efforts discussed in *Fernando et al.* [1998], *Lozovatsky and Ksenofontov*, [1998], and *Lozovatsky et al.*, [1998].

The results of this part of the project have been published by *Lozovatsky et al.* [2001] and presented at the Ocean Science Meetings (San Diego, 1998 and Honolulu, 2002) and XXIII IUGG General Assembly, (Birmingham, UK, 1999).

B. Mixing on a Shallow Non-Tidal Shelf

The aim of this part of the project was to estimate eddy diffusivities and variables characterizing turbulent mixing on the shallow (depth < 30 m) shelf. The data analysis was based on the measurements taken on the Black Sea shelf near the Bulgarian coast. Of particular interest was to identify major microstructure layers (features) of different states of evolution and to study the turbulent scales (e.g. Thorpe scales) within them. Vertical profiles of temperature, conductivity and small-scale shear were measured over the entire water column over a NW to SE transect across the shelf using free-falling microstructure profiler BAKLAN-S [*Paka et al.* 1999]
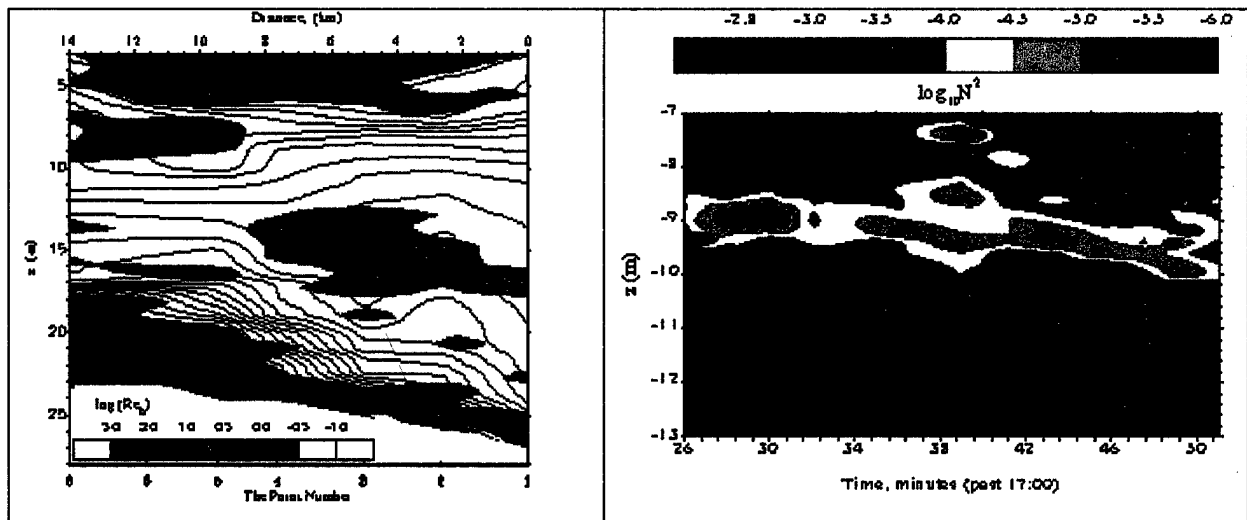
Fig. B1. *Left Panel*: The buoyancy Reynolds number across the shelf; brown-red regions correspond to UBL, BBL, AP, and STZ; SIL is shown in yellow. The green-blue areas adjusted to the upper and bottom boundary layers represent DPC and ITPC. *Right Panel*: Quasi-homogeneous patch (green-yellow area), which includes well-mixed active patches (brown-red areas). A stratified layer shown in dark-blue colors coincides with the microstructure displacement patch.

Five principal hydrodynamic layers (the upper and bottom boundary layers, UBL and BBL, separated by a weakly-turbulent inner stratified layer (SIL) and sharp diurnal and main pycnoclines DPC and ITPC), and five transient (secondary) microstructure features (active (AP), quasi-homogeneous (QHP), and stratified dissipative (SDP) turbulent patches, shear turbulent zone (STZ) and microstructure displacement patch (MDP)) embedded in the principal layers were identified (Fig. B1). The delineation of these layers was based on the buoyancy frequency N, dissipation rate of the turbulent kinetic energy ε, buoyancy Reynolds number $Re_b = \varepsilon/30\nu N^2$ and the Thorpe displacements d'.

The measurements were used to calculate such quantities as the mass diffusivity, K_N, scalar diffusivity, K_{sc}, the mixing efficiency, γ, the patch thickness h_p as well as the Thorpe lengthscale L_{Th}. The probability distribution function for the ratio L_{Th}/h_p was found to be lognormal for QHP, AP and MDP. The median values of L_{Th}/h_p distributions varied over a decade from 0.027 to 0.35 depending on the state of turbulence (mixing Reynolds number, $R_m = K_{sc}/\nu$) and stratification (patch Richardson number, $Ri_p = N^2 h_p^4/K_{sc}^2$). Higher values of L_{Th}/h_p were associated with regions of active, fully-developed turbulence. On dimensional grounds, L_{Th}/h_p was proposed to be a nondimensional function P^* of R_m and Ri_p:

$$\hat{L}_{Th} \equiv \frac{L_{Th}}{h_p} = P^*\left[\frac{\hat{L}_{Th}^{max}}{\left(1+Ri_p/60\right)^{1/4}\left(1+150/R_m\right)}\right] \equiv P^*(x),$$

which correlates well with present observations along with those of *Dillon* (1982) and *Gibson et al.* (1993), for $P^*(x) = 0.03 + 1.5x$ and $\hat{L}_{Th}^{max} = 0.3$ (Fig. B2, left panel). The ratio L_{Th}/h_p is an increasing function of R_m when $R_m < 150$ and tends to be a constant for $R_m \gg 150$. For a constant R_m, L_{Th}/h_p decreased with Ri_p.

It was also shown that the correlation between eddy and scalar diffusivities K_N and K_{sc} strongly depends on space-time averaging. For domain-averaged diffusivities, $\hat{K}_{sc} \approx \hat{K}_N$, for $\hat{K} \geq 10^{-5}$ m^2/s (Fig. B2, right panel) and a mixing efficiency $\hat{\gamma} \approx 0.2$. The domain-averaged diffusivities vary in the range $(0.4-4.0)\times 10^{-4}$ m^2/s in the bottom and surface boundary layers and shear turbulent zone. In sharp pycnoclines, it assumes values of $(1-2)\times 10^{-6}$ m^2/s.
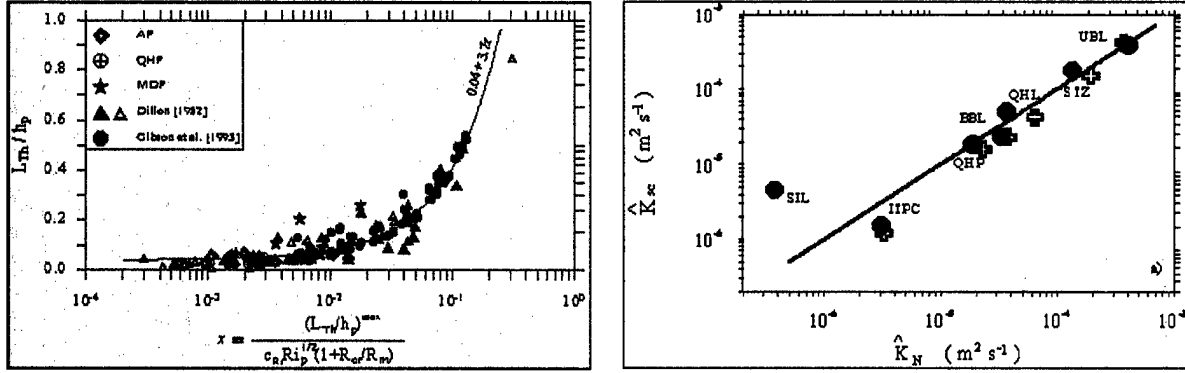
Fig. B2. *Left Panel*: The dependence of the normalized Thorpe scale on Ri_p and R_m numbers fitted by (1) with a_o = 0.04. The coefficient of determination is 0.8. *Right Panel*: The relationship between eddy and scalar diffusivities averaged for several representative regions of the water column. The straight line is a linear dependence $K_{sc} = K_N$.

Based on these representative values of $\hat{K}$ in various layers, an overall water-column averaged vertical eddy diffusivity on the shelf was evaluated as $\langle K \rangle = (9-11) \times 10^{-5}$ m²/s. Despite the lack of data in the upper 3 meters of the water column (about 10% of the total shelf depth), the above value can be used to characterize overall mixing on the shallow shelf of the Black Sea in the beginning of the autumn, where the winds are moderate and multi-layered density stratification is well established. Nevertheless, significant variation of $\hat{K}$ with depth shows that the column-averaged diffusivity $\langle K \rangle$ is not an appropriate measure for the computation of vertical transports through the thermocline. The depth-dependent, layer-averaged diffusivities $\hat{K}$ rather than $\langle K \rangle$ should be considered for computation of vertical transports in shelf waters.

The results of this study have been published by *Lozovatsky et al.* [1999], *Lozovatsky and Fernando* [2000], and *Lozovatsky and Fernando* [2002] and presented at 29th International Colloquium on Ocean Hydrodynamics, (Liege Belgium, 1997), International Symposium on Oceanic Fronts and Related Phenomena, (St. Petersburg, Russia, 1998), and XXIII IUGG General Assembly, (Birmingham, UK, 1999).

C. Internal Waves and Thermocline Splitting at a Tidally Affected Shelf Break

Profiling and mooring measurements have been carried out in the coastal zone of the Peter the Great Bay of the Sea of Japan to study internal wave dynamics on a tidally affected shelf.

8

The generation of internal waves with wavelengths of 1 - 2 km in the background of a thermocline rising near the shelf break can be seen at two transects taken offshore (T7) and onshore (T8) (region A in Fig. C1,a) taken close to the spring tide.
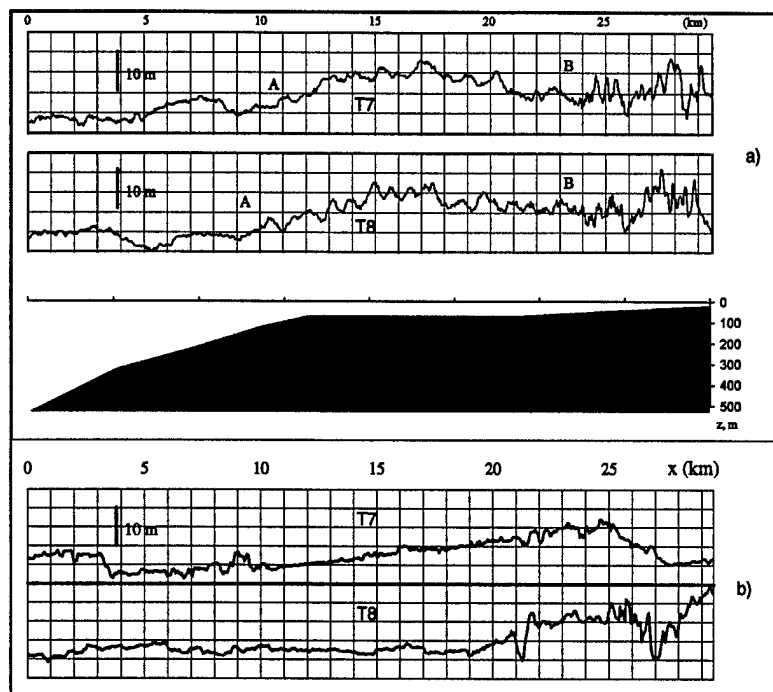

Fig. C1.   The thermocline displacements measured at the offshore (T7) and onshore (T8) transects across a small canyon near the shelf break. The coastline is about 8 km from the ending point at $x = 29.5$ km.

Sharp changes in the amplitudes and wavelengths of vertical displacements in region B at the both transects clearly indicate the transformation and secondary generation of small-scale internal waves on the shelf. Shortening of the wavelengths from the shelf break towards the coast is accompanied by growth of wave amplitudes. A similar transformation of internal waves on the California shelf has been reported by *Pringle* [1999].

Towing measurements at the same transect, T7 and T8, have been repeated during the neep tide. The displacements of thermocline registered therein (Fig. C2,b) are highly inhomogeneous. The highest amplitudes of fluctuations were also found over the shelf close to the coast $(23 < x < 28$ km in Fig. C1,b); less prominent internal waves were measured while traversing the shelf break and canyon $(x < 10$ km). The central segments of these records $(10 < x < 20$ km) are almost free of internal waves. The difference between internal wave records shown in panels a) and b) of Fig. C1 can be associated with the differences in the intensity of tidal oscillations before perigee of the Moon (Fig. C1,a), which is close to the maximum tidal forcing, and almost

9

in the Moon apogee (Fig. C1,b) corresponding to low tides and low-amplitude internal waves. Therefore, tidal variability is an important factor of the intermittency of internal wave generation at the shelf break of the Peter the Great Bay.

It was observed that a narrow horizontal seasonal thermocline occupying the depth range between 20 and 40 m in the open sea deepens significantly upon approaching the shelf break. Sometimes this sharp thermocline thickened over the shelf break with further splitting into two new interfaces. In Figure C2, we show the temperature contour plot taken in summer time along $132^0 05$'E across the shelf break.
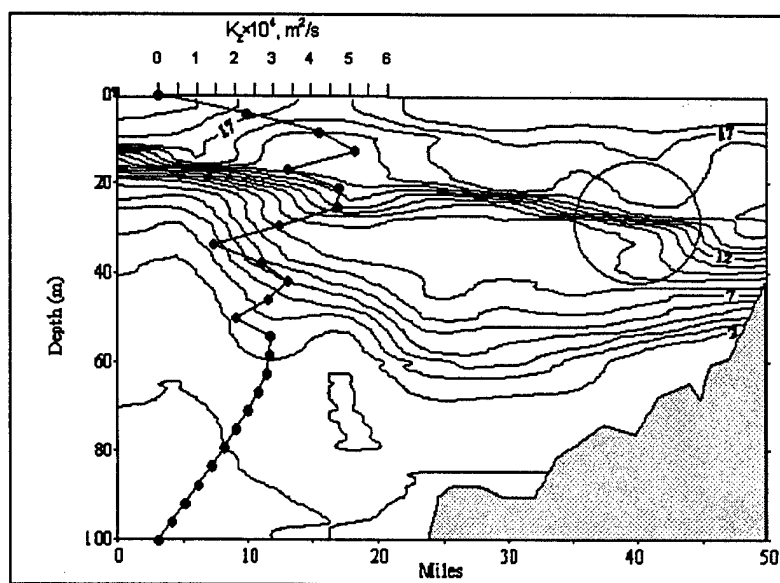

Fig. C2. Temperature contour plot across the slope and shelf boundary. The region of secondary splitting of the thermocline is marked by circles. The dotted line is the vertical profile of the estimated diffusivity $K_z(z)$. The local maxima in the depth ranges 15-25 m and 40-45 m correspond to the regions of thermocline splitting.

The striking feature in this plot is the thermocline splitting near the shelf break that can be seen at $x = 10 - 15$ miles. For the lower part of the water column ($T < 7^{\circ}C$), the isolines go down from $z = 20$ m at $x = 0$ to $z = 55 - 65$ m near the shelf break, where $x = 22$ miles (Fig. C2). A core of the thermocline ($T = 9 - 14^{\circ}C$) remains almost at the same depth gradually deepening towards shallow waters. The upper part of thermocline ($T > 15^{\circ}C$) ascends forming a dome of cooler water in the upper 20-meter layer over the shelf break. The secondary splitting of the upper stable sub-layer can be seen in the right part of the section at $x = 35 - 40$ miles. The amplitudes of relatively short-period internal waves are considerably amplified in the regions of thermocline

10

splitting. Secondary splitting of the sub-layers with higher gradients occurred several miles shoreward from the shelf break. It was suggested that deformations of the thermocline are associated with a hydraulic jump that originates over the continental slope at the distances of 5-15 miles from the shelf break. This scenario is supported by numerical modeling of internal wave generation on the shelf in print [*Navrotsky et al.* 2002a].

As observed, amplification of internal wave amplitudes sometimes coincide with regions of the thermocline splitting, which is presumably caused by turbulent mixing resulting from the energy cascade in non-linear internal waves over the shelf. To estimate vertical diffusivities K_z that could be associated with the wave-induced mixing, *Navrotsky* [1999] suggests that in a horizontally-inhomogeneous ocean $K_z = -Q_z/\partial \overline{T}/\partial z$ (where Q_z is vertical heat flux and $\partial \overline{T}/\partial z$ the vertical component of mean temperature gradient) can be specified of the wave amplitude A, its vertical derivative A', the slope of isopycnal or isothermal surfaces $tg\beta$, and the phase velocity c_{ph}, as

$$K_z = \frac{1}{2}A'A c_{ph} tg\beta .$$

The data collected at the shelf break of the Sea of Japan allow estimating K_z that could be generated by internal waves with 4-5 m amplitudes and 1400-2000 m wavelengths that represent a combination of two modes $\omega_1 = 2\pi/(2.5\times10^3)$ s^{-1} and $\omega_2 = 2\pi/(7\times10^3)$ s^{-1}. The phase speed for these waves calculated numerically from the dispersion relation is 0.6-0.7 m/s for the first mode and ~ 0.32 m/s for the second mode. The mean slope of thermocline in front of the shelf break varies in the range $(2 - 4)\times10^{-3}$. To calculate $K_z(z)$, we also need to know vertical derivatives of the wave amplitudes, which can be obtained from profiles for the first and second normal modes (not shown here). For a combination of these two modes the overall effect of wave-induced mixing can be characterized by $K_z = K_z1 + K_z2$. This profile is given in Fig. C2 in the background of temperature transect where thermocline splitting is observed. The major maximum of $K_z = 5.2\times10^{-4}$ m^2/s is in the upper stratified layer and a lesser secondary maximum $(3.7\times10^{-4}$ m^2/s) is in the lower thermocline (the depth range 35 - 45 m). This can explain why we observed the secondary splitting only in the upper thermocline (shown by a circle in Fig. C2), but not in the lower one. The estimates of diffusivities given above are conservative. The numbers could be at least twice as much for larger β; the wave amplitudes exceeding 5 m are also common case on this shelf. The obtained estimates of K_z are in a good agreement with those found by *Inall et al.*

[2000] on Malin shelf. These authors suggest the averaged $<K_z> = 2 \times 10^{-4}$ m^2/s in the thermocline over the shelf that could be associated with disintegration of tidal internal wave and generation of packets of high-frequency nonlinear internal waves during neap tide. The diffusivities may go up to 13×10^{-4} m^2/s during spring tide. Our estimates of K_z on the shelf in the Peter the Great Bay fall in this range. Note, that in enclosed and semi-enclosed seas with low tidal forcing (like Black and Baltic Seas, for example), the diffusivities in the thermocline are usually significantly smaller than the numbers obtained by *Inall et al.* (2000) and those reported above. In sub-section B, we showed that on a shallow Black Sea shelf, even within the active turbulent regions in the pycnocline, the diffusivities do not exceed 1.5×10^{-4} m^2/s (generally constrained by an upper limit of 2×10^{-5} m^2/s). This is about an order of magnitude lower than the numbers obtained for the shelf of the Peter the Great Bay. This emphasizes a significant role of tidally forced internal waves in the generation of buoyancy flux and formation of vertical fine structure on tidal shelves.

The results of this research have been presented at the 2001 TOS Meeting in Miami Beach, Florida and submitted for publication to *CSR* [*Navrotsky et al.* 2002b].

D. Spatial Decay of Topographically Induced Internal Tides and Ocean Mixing

The spatial decay of energy density of tidal internal waves (TIW) was studied using field measurements and a numerical model. The data have been taken in the Indian Ocean near the Mascarene Ridge and in the Canary Basin of the Eastern Atlantic near the Heyres-Irving-Cruiser chain of seamounts. Several moorings were deployed at distances between 90 and 1745 km east of these topographic features, with instruments located in the depth range 500 – 2500 m. The energy densities of TIW averaged over the spring-neap cycle were calculated using semidiurnal tidal components of current and temperature time series as well as local vertical gradients of temperature and density.

It was found that the horizontal component of TIW, E_H, is less depth-dependent compared to the vertical component, E_ζ ; both components, however, showed a general decrease of magnitude with the distance from topography. Internal tidal waves lose approximately half of their total energy density $E_{TW} = E_H + E_\zeta$ energy at every wavelength λ of the first mode over a distance between $x/\lambda = 0.6$ and 12 from the ridge. The role of TIW in the energetics of oceanic internal wave field becomes insignificant (less than 10% of the total internal wave energy of the

12

Garrett-Munk model) beyond about 1500-1700 km from the ridge, which is equivalent to (10-12)λ. Numerical calculations carried out by *Holloway and Merrifield* [1999] on the propagation of TIW away from the Hawaiian Ridge showed that the TIW energy density becomes less than that of the barotropic tide at a distance of 400 km from the source, which is approximately 3λ. Our observations east of the Mascarene Ridge revealed a longer distance of TIW propagation ($x = 10\lambda$). The dependence of the normalized energy density of TIW on distance from the topography (Fig. D1) can be approximated by a power law $E_{TW}/E_{GM} = 2.2 \times (x/\lambda)^{-1.2}$, which indicates much faster spatial decay of the TIW energy than that suggested by *Morozov* [1995].
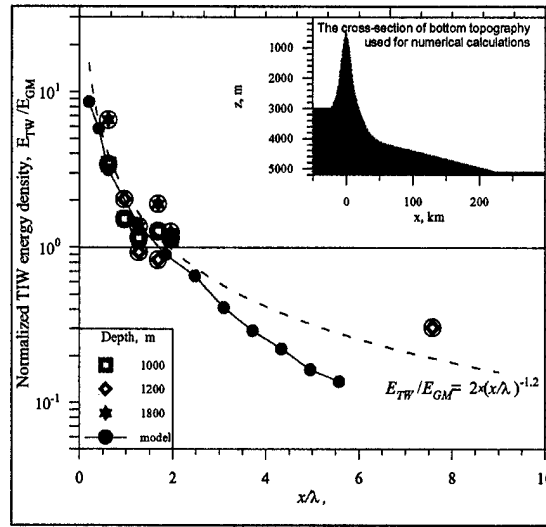

Fig. D1. A comparison between model calculations of the TIW energy density normalized by the GM energy E_{GM} at $z = 1200$ m (solid dots) and the observations east of Mascarene Ridge at $z = 1000 - 1800$ m. The geometry of the bottom relief used for calculations is in the insert.

To simulate the spatial decay of TIW energy density generated by barotropic tide near the Mascarene Ridge, we used an modified version of the non-hydrostatic, non-linear two-dimensional numerical model described in *Morozov and Vlasenko* [1996]. The numerical calculations show that for $x/\lambda < 2$-3 the decrease of TIW energy density is similar to the observations (Fig. D1). The spatial decay beyond these distances is faster than that observed from the data, and the model predicts $E_{TIW}/E_{BT} = 1$ at $x = 5.5\lambda$, which is somewhat closer to that obtained by *Holloway and Merrifield* [1999]. The rapid decay predicted by the model can be attributed to many reasons, including the possibility that the bed roughness can serve as an additional source of internal tide generation, which is not accounted in the model.

We evaluated mixing induced in the thermocline by TIW using internal-wave dissipation estimates based on [*McComas and Muller* 1981] model. A rough estimate of turbulent diffusivities associated with TIW energetics suggests a mass diffusivity of $K_N \approx (1\text{-}2)\times10^{-4}$ m^2/s in the main pycnocline at a distance of $x = 100$ km from the ridge. The diffusivity decreases to $(0.5\text{-}1.1)\times10^{-5}$ at $x > 1000$ km, approximately as x^{-1} (Fig. D2).
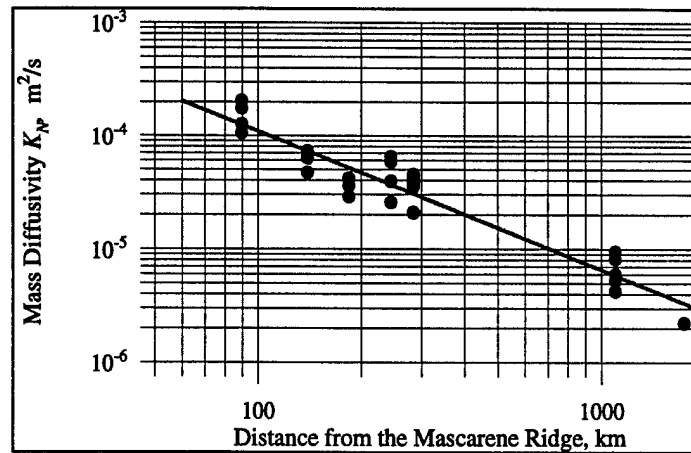

Fig. D2. Vertical diffusivities at various distances from the Mascarene Ridge based on the dissipation estimates made using *McComas and Muller* [1981] model.

The energy generated at the ridge, therefore, may lead to a significant enhancement of vertical diffusivity (by a factor 3-5 for $x < 300$ km from topography) beyond the typical background value of the main oceanic pycnocline 10^{-5} m^2/s. Our analysis suggests possible enhancement of turbulent mixing due to internal tides up to distances 1000 km from the topography.

The results obtained have been partially presented at the Ocean Science Meeting in San Antonio (2000), published in *Lozovatsky et al.* [2000], and submitted for publication to JGR-Oceans [*Lozovatsky et al.* 2002, under revision].

E. Modeling of Step-Like Structure in the Pycnocline

We have developed a detailed numerical model of a rotating, stratified and sheared turbulent boundary layer. This model can produce a series of fine-scale quasi-homogeneous layers in a pycnocline of constant buoyancy frequency N_0. Numerical experiments were run with small-scale parameterizations written in the following form:

14

$$K_N/K_M = 1/(1 + Ri/Ri_{cr}), \quad K_M = K_{Sh}/\sqrt{1 + Ri/Ri_{cr}}$$

where K_N is the mass diffusivity, K_M is the eddy viscosity and K_{Sh} is the shear-dependent eddy viscosity in non-stratified flows. This parameterization ensures instability of density gradients in a stably-stratified layer with decreasing buoyancy flux F_b, when N^2 exceeds a critical value, corresponding to a local maximum of $F_b(N^2)$. This type of instability was proposed by *Phillips* [1972] and *Posmentier* [1977] and later treated by several others. It was also found, that the development and decay of fine structure are strongly dependent on inertial oscillations, which enhance vertical shear at the density interfaces between homogeneous layers locally. As a result, the local Richardson numbers decreases, thus generating shear-induced turbulence within interfaces. This is why some of the interfaces are rapidly destroyed and fine structure may even vanish at times, as can be seen in the Fig. E1, where we present an example of calculations for a constant wind-induced friction velocity of 0.9 cm/s, linear initial stratification, $N^2 = 2.5 \times 10^{-5}$ s^{-2}, and Coriolis parameter $f = 10^{-4}$ s^{-1}. The layering phases alternate with periods during which the steps vanish completely. These no-layering stages may last up to (0.5 - 0.9)$\times T_{in}$, where T_{in} is the inertial period.
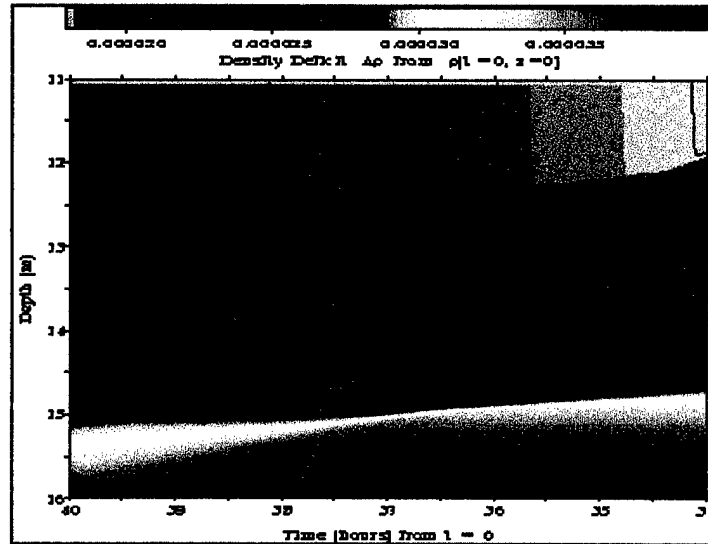

Fig. E1. The generation and decay of density steps in the upper pycnocline at the end of the 2nd inertial period ($T_{in} =$ 17.45 h), counting from the beginning of computation.

The rotation effect leads to a later development of the steps in the pycnocline at low latitudes (Fig. E2). The lifetime of these structures is longer compared to higher latitudes.
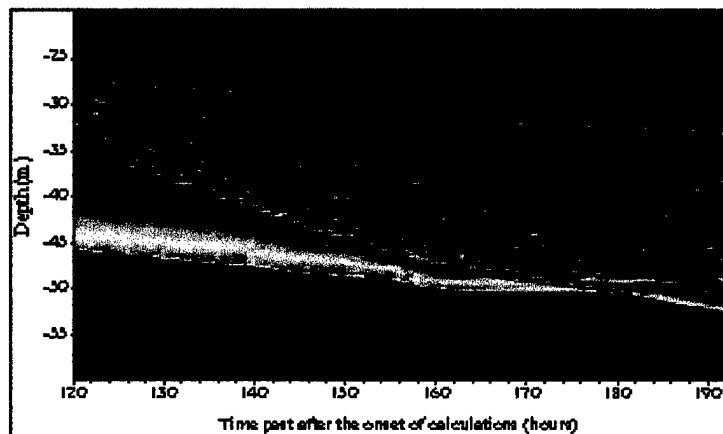

Fig. E2. Density interfaces simulated in the low-latitude pycnocline ($f = 10^{-5}$ s^{-1}) below well-mixed upper quasi-homogeneous layer. Initial linear density profile has a gradient $d\rho/dz = 2.5 \times 10^{-8}$ g/cm^3, $u_* = 0.9$ cm/s.

Another example of the development of fine structure in the near-bottom boundary layer is shown in Fig. E3. These calculations were targeted to simulate the density fine structure on the West Sahara shelf during the development of a quasi-homogeneous turbulent bottom boundary layer from a linear density profile influenced by a tidal current with semidiurnal and diurnal constituents.
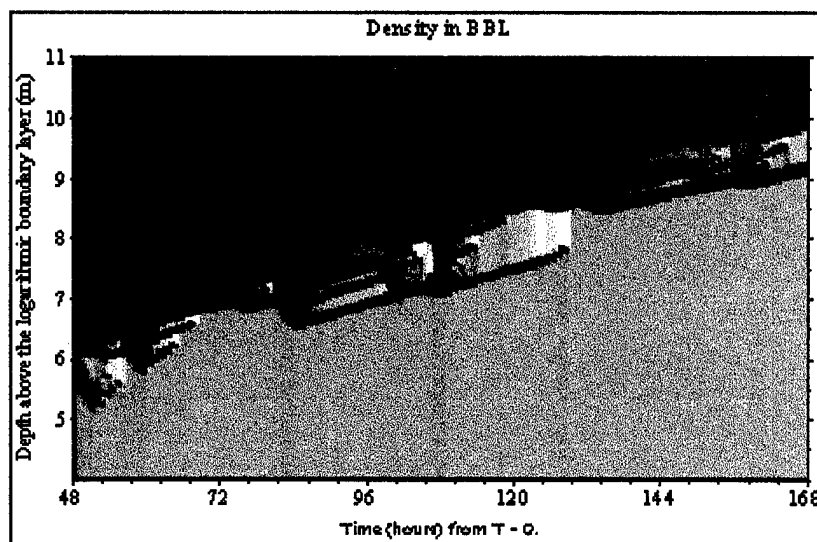

Fig. E3. The appearance of a series of fine-scale homogeneous layers and density interfaces in the near-bottom pycnocline

16

It was found that a small, but sustained, background shear is required to generate the steps. This minimal shear Sh_o corresponds to a background bulk Richardson number Ri_o close to 6, and this criterion limits the steps generation in the model. This may indicate that, only in the regions with pre-existing global $Ri < Ri_o$, intermittent step-like structure can be generated in stably stratified waters under synoptic variations of wind stress (or tidal-induced bottom stresses).

Preliminary results of this study have been presented at The Johns Hopkins Conference in Environmental Fluid Mechanics (Baltimore, 1998) and XXIII IUGG General Assembly, (Birmingham, UK, 1999) and published in *Fernando et al.* [1998], *Lozovatsky and Ksenofontov* [1998], and *Lozovatsky et al.* [2000,b].

G. Fine Structure and Diapycnal Mixing in the Equatorial Atlantic

Using CTD profiling data obtained in the equatorial Atlantic during the 8th cruise of R/V "Akademik Ioffe" along a trans-Atlantic section [*Lappo et al.* 2000], we analyzed predominant thermohaline fine structures associated with various water masses of different origins. Below the upper 500-meter layer, the following major water masses were identified: Antarctic Intermediate Water (AAIW, $600 < z < 1400$ m), North Atlantic Deep Water (NADW, $1400 < z < 3700$ m) and Antarctic Bottom Water (AABW, $z > 4100$ m). The bottom and upper boundary layers at this transect contained mostly step-like fine structure whereas the intermediate waters were full of intrusions. Examples of potential temperature, density, and salinity profiles for the main water masses are shown in Fig. G1. Waters of the Antarctic origin (Fig. G1,a,d) are richer in fine structure compared to North Atlantic waters (Fig. G1,b,c). There are only weak fine structure details in Fig. G1,c that are most likely caused by internal waves in mid-NADW. A few quasi-homogeneous layers and temperature inversions with a thickness of 10-20 m can be identified in Fig. G1,b. These elements of the upper NADW are associated with a salinity maximum of Mediterranean origin. Stable salinity stratification prevents double-diffusive convection here. On the contrary, estimates of stability parameter R_ρ showed that salt-fingering is a possible mechanism of step-like structure formation in the upper AAIW (Fig. G1,a). In the lower AAIW ($z > 800$ m), intrusive fine structure is most likely formed due to isopycnal advection because inversions in temperature and salinity compensate each other in density profiles. Intrusions in

AAIW are tied to the boundary between AAIW and the Upper water of the Circumpolar Current. It is likely that the generation of fine structure at this boundary increases the rate of exchange of thermohaline properties, thus further reducing disparities in T,S characteristics.
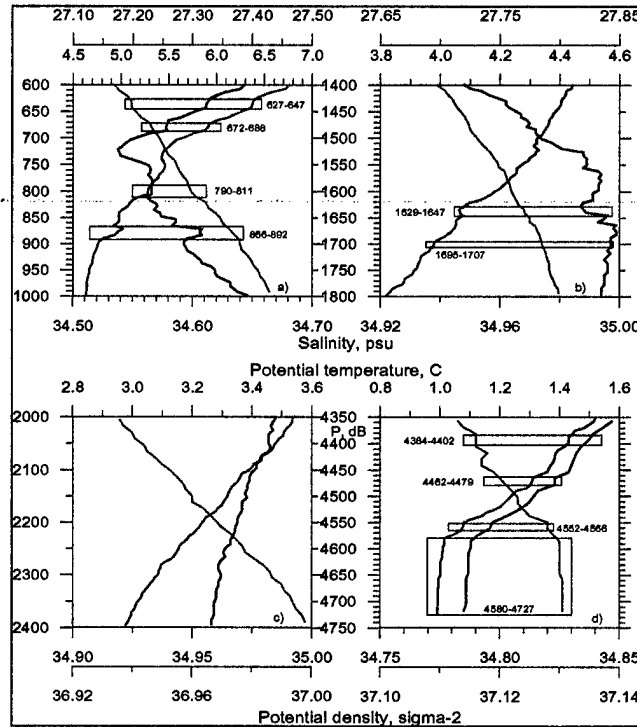

Fig. G1. Typical fine structures associated with major waters of the Equatorial Atlantic: intrusive - AAIW (a) and upper NADW (b), weak internal wave induced irregularities – mid-NADW (c), and step-like structure of turbulent origin - AABW (d).

The Antarctic Bottom Water contains predominantly step-like fine structure (Fig. G1,d). Several steps with thickness from 14 to 18 m can be seen above approximately homogeneous 150-meter near bottom boundary layer. These layers cannot be of salt-finger origin given the high mean density ratio (R_ρ = 5) there. The bottom water flows toward the equator along relatively narrow channels. Mixing due to bottom and lateral boundary roughness explains why a thick homogeneous layer appears near the bottom and how quasi-homogeneous steps can be formed in the overlaying pycnocline due to boundary mixing. A numerical model was developed to describe the generation of such step-like structure [*Lozovatsky et al.* 2000b]. The formation of prominent fine structure in the bottom boundary layer enhances the changes of water properties of AABW when it moves north, in contrast to slow transformation of the overlying NADW moving south.

18

Analysis of thermohaline sections and mesoscale fluctuations of potential temperature θ and salinity S in and above the core of AAIW, which occupies the depth range 750 - 850 m, revealed the possibility of diapycnal upwelling of AAIW into the upper layers west from the Mid-Atlantic Ridge. The contour plots of potential density $\sigma_{0.7}$ calculated for the reference pressure 700 db (the upper panel) and the dependences of salinity and potential temperature $\theta_{0.7}$ upon $\sigma_{0.7}$ along the western part of section AI-2000 (the middle and lower panels) are shown in Fig. G2. The ascend of temperature and salinity contours is seen from approximately 41.5° to 45.5°W in the density range $\sigma_{0.7} \approx 30.52 - 30.22$, which indicates a diapycnal transformation of water properties in the depth range 300 - 800 m (see the location of $\sigma_{0.7} \approx 30.52 - 30.22$ in the upper panel). It is important to emphasize that in this region the density contours are stretched not only upwards but also downwards, revealing a relatively low-stratified volume of AAIW at unusually shallow depths. The transformation can be caused by diapycnal mixing (turbulence
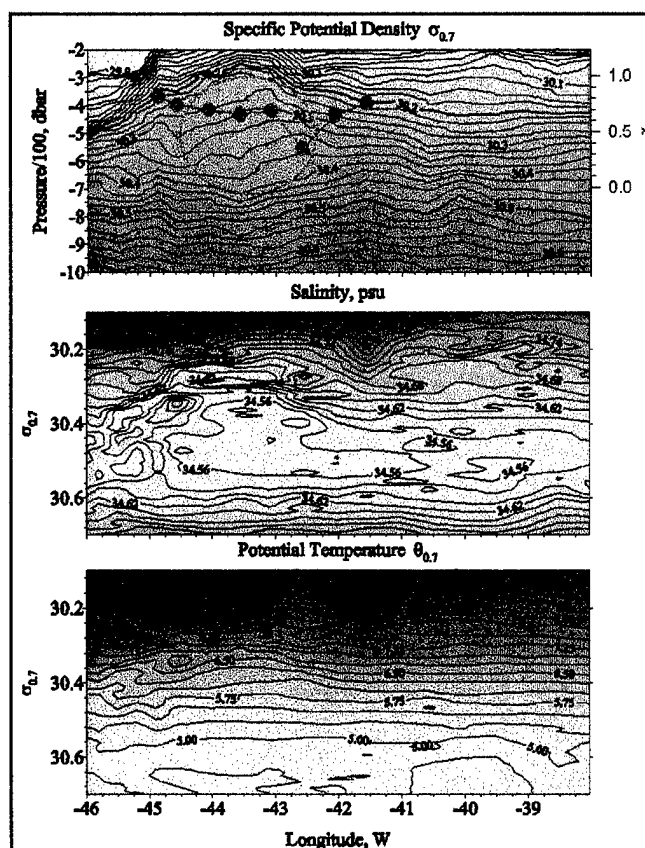

Fig. G2. The contour plots of $\sigma_{0.7}(P, \lambda)$, $S(\sigma_{0.7}, \lambda)$, and $\theta_{0.7}(\sigma_{0.7}, \lambda)$. The ellipse marks a region of stretching density contours, indicating a lower stratification due to possible mixing. The "transformation" parameter γ is in the upper panel.

19

and salt finger convection from above) or by lateral mixing associated with horizontal advection. To quantify the relative contribution of vertical advection (including mixing) compared to horizontal (isopycnal) advection, we use the so-called "transformation" parameter

$$\gamma = \frac{A_S}{A_\theta}\frac{\partial\theta/\partial z}{\partial S/\partial z} - 1 \left/ \frac{\alpha}{\beta}\frac{\partial\theta/\partial z}{\partial S/\partial z} - 1\right.$$

Here A_S and A_θ are characteristic amplitudes of salinity and temperature inhomogeneities in a layer under consideration. In the case of isopycnal motions $\gamma = 1$; for vertical motions, $\gamma = 0$. The estimates of A_S and A_θ were taken as the r.m.s. of θ and S fluctuations in the depth range 300 - 700 m, which is above the core of AAIW. The "transformation" parameter γ, which is shown in the upper panel, is in the range 0.31 – 0.62 within the green circle, growing to 0.82 – 0.85 outside. This signifies that diapycnal mixing is responsible for at least 40% of the observed transformation of AAIW properties. More detailed analysis is required to separate contributions of turbulent mixing and double diffusion to the diapycnal transport of AAIW. The present study shows that the region of diapycnal upwelling of AAIW is not limited by the western part of the South Atlantic but extends also to the Northern Hemisphere, influencing the rate of compensation of fresh water losses is the North Atlantic.

Results of this portion of the project have been reported at the IAPSO General Assembly in Mar del Plata (Argentina, 2001) and published in *Lappo et al.* [2001] and *Lozovatsky et al.* [2003].

F. Oceanographic Data Bases

The mooring database of the P.P. Shirshov Institute of Oceanology Rassian Academy of Sciences (SIO RAS) has been created. The basic information on data files is arranged in tables. An example is shown below.

North Atlantic, South of Iceland.

Filename	Buoy number	Measurements start on	Sampling interval	Duration	Latitude	Longitude	Instrument depth	Seafloor depth	Parameters
isl--1-1.dat	1	17.08.1989 00-00	60 min	77 h	54 09 N	26 44 W	1000	3366	U V T
isl--1-2.dat	1	17.08.1989 00-00	60 min	317 h	54 09 N	26 44 W	1500	3366	U V T

The data files are in ASCII format. Each file contains time series of current components U and V and temperature T along with supplementary information in the WOCE standard format. The data are sorted by the name of the experiment, region and year. The database and a search system are currently linked to the web page of Environmental Fluid Dynamics Program of Arizona State University *http://www.eas.asu.edu/~pefdhome*. The data files can be easy opened or downloaded at *http://ceaspub.eas.asu.edu/oceanrus/SIOMOOR/welcome.htm* using a clicking map (Fig. F1).
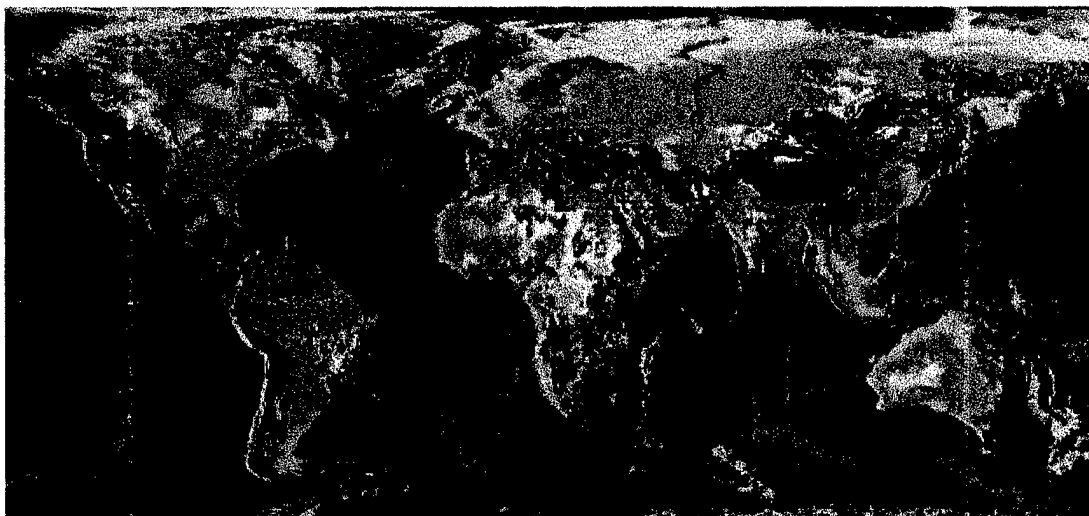

Fig. F1. The map of SIO RAS mooring database. The measurement sites are shown by dots.

The CTD data of several expeditions in the South China Sea, Sea of Japan, and Okhotsk Sea have been retrieved from the archives of the Pacific Oceanological Institute (Vladivostok), examined for the data quality control and assurance and posted to the EFDP web site with direct access via *http://ceaspub.eas.asu.edu/oceanrus/FarEast/welcomeN.htm* .

The oceanographic database on the EFDP web site was extended to include new measurements taken in 1999 and 2000 during two trans-Atlantic coast-to-coast sections along approximately 48°N and 7°N respectively. The later include CTD data obtained. The data can be accessed at *http://www.eas.asu.edu/~pefdhome/Research/Ocean/oceanfld.htm* via clicking maps. Descriptive analyses of main thermohaline features are also given in conjunction with each transect presented on the web.

The oceanographic database will be upgraded in the near future by including the new CTD measurements collected in 2001 during the 9th cruise of R/V "Akademik Ioffe" at trans-Atlantic section along 53°N. It is planned to conduct future updates in cooperation with oceanographers from SIO RAS.

COLLABORATION

We have close collaboration with oceanographers from the Former Soviet Union (Drs. E. Morozov, S. Shapovalov, V. Navrotsky, and A. Ksenofontov) who are active in studying turbulence, internal waves and mesoscale oceanic dynamics. During the project period, three oceanographic cruises across Atlantic were organized in cooperation with P.P. Shirshov Institute of Oceanology, Russian Academy of Sciences, allowing obtaining of unique new data sets of CTD and ADCP measurements, which are incorporated to the Oceanographic Database developed at the EFDP ASU web site. International contacts were maintained with scientists from Canada (Dr. K. Kreyman, McMaster University) and Spain (Dr. Elena Roget, University of Girona) to measure and analyze turbulence in the upper boundary oceanic layer and near-surface atmospheric layer.

EXECUTIVE SUMMARY

The generation and evolution of small, fine, and meso-scale structures in deep and littoral oceans were studied using field observations, data analysis and numerical simulations. The data have been collected by oceanographers from the Former Soviet Union, the archives of which were scrutinized for data quality, used for our own research and posted on the web site for the use of international scientific community. Three additional new trans-Atlantic cruises were organized during the project period in collaboration with the P.P. Shirshov Institute of Oceanology, Russian Academy of Sciences. Close collaboration was maintained with Russian and Spanish scientists with regard to conducting field measurements and data analyses.

The influence of topography on oceanic flows was investigated on shelves and continental slopes, around seamounts and near submarine ridges. The generation and amplification of internal tides near the ridges were evaluated using moored measurements and

22

CTD transects. The excessive energy of tidal internal waves was found to produce enhanced mixing in pycnocline at a distance up to 1000 km from the topography. The generation of extensive turbulent "columns" was discovered above the seamount summits. The diffusivities in these "columns" and in turbulent bottom boundary layers above the flanks of seamounts can exceed the background values by at least two orders of magnitude. Shelf induced mixing was studied using data from semi-enclosed seas with (Peter the Great Bay of the Sea of Japan) and without (Black Sea) tidal influence. Spatial distributions of key turbulence and wave quantities were evaluated whenever possible and parameterized. For example, we obtained a formula describing the dependence of the normalized Thorpe scale on the mixing Reynolds and patch Richardson numbers. The need for accurate process-orientated division of water column in calculating the diffusivities (because of layering) was clearly demonstrated. The vertical diffusivity in the pycnocline of a non-tidal shelf was found to be close to 2×10^{-5} m^2/s, while on the tidally influenced shelf, where the evolution of fine structure was correlated with the intensity of tidal forcing, the nature of topography and stratification, the diffusivities are 5-10 times higher due internal-wave induced mixing on the shelf break. Numerical modeling efforts were focused on reproducing the structure of the thermocline evolution and internal wave phenomena, both on the shelf and in deep waters, in part based on parameterizations developed during this research project. The generation of step-like structures within the pycnocline influenced by boundary forcing and rotation was found to be dependent on a critical background shear in regions under consideration. Accurate high-fidelity parameterization of turbulent mixing generated near topography is crucial for modeling of mesoscale oceanic dynamics and large-scale circulation.

PUBLICATIONS related to the PROJECT

Fernando, H. J. S., J. S. R. Hunt, E. J. Strang, A. L. Berestov, and I. D. Lozovatsky, "Turbulent mixing in stably stratified flows: limitations and adaptations of the eddy diffusivity approach", In: *"Physical Processes in Lakes and Ocean"*, Coastal and Estuarine Studies, **54**, AGU, 351-362, 1998.

Fernando, H.J.S., and I.D. Lozovatsky, "Turbulence and mixing in oceans", *Proc., 6th Workshop Phys. Proc. in Natural Waters* (Ed. X.Casamitjana), UdG, Girona, Catalonia, Spain, 1-13, 2001.

Lozovatsky, I. D., and A. S. Ksenofontov, "Modeling of atmospheric forced mixing on the shallow shelf", In: *"Physical Processes in Lakes and Ocean"*, Coastal and Estuarine Studies 54, AGU, 111-118, 1998.

Lozovatsky, I. D., T. M. Dillon, A. Yu. Erofeev, and V. N. Nabatov, "Variations of thermohaline structure and turbulent mixing on the Black Sea shelf at the beginning of autumn cooling", *J. Marine Systems*, 21, 255-282, 1999.

Lozovatsky, I. D., and H. J. S. Fernando, "Turbulence in stratified patches on a shallow shelf", In: *"Oceanic Fronts and Related Phenomena"*, IOC Workshop Report Ser., No.159, 314-319, 2000.

Lozovatsky, I.D., E.G. Morozov, and V.G. Neiman, , "Decay of the energy of internal tidal waves generated near submarine ridges. *Doklady Earth Sciences*, 375(2), 245-248, 2000a.

Lozovatsky, I.D., Ksenofontov, A.S., and Fernando, H.S.J., The formation of step-like structure in near surface and near-bottom pycnoclines", *Stratified Flows II*, (Ed. G. Lawrence, R. Pieters, N. Yonemitsu), UofBC, Vancouver, Canada, 1215-1220. 2000b.

Lappo S.S., I.D. Lozovatsky, E.G. Morozov, A.V. Sokov, and S.M. Shapovalov, "Variability of water structure in the equatorial Atlantic", *Doklady Earth Sciences*, 379(5), 686-690, 2001.

Lozovatsky, I.D., E.G. Morozov, E. Roget, and S.M. Shapovalov, "Ocean mixing influenced by topography," *Proceed. 3rd Int. Symp. Environ. Hydr.*, CD-ROM Mira Digital Publ., 6p., 2001.

Lozovatsky, I. D., and H.J.S. Fernando, "Turbulent mixing on a shallow shelf of the Black Sea", *J. Phys. Oceanogr.*, 32(3), 945-956, 2002.

Lozovatsky, I.D., E.G. Morozov, H.J.S. Fernando, "Spatial decay of energy density of internal tides", *JGR-Oceans*, 2002, (under revision).

Lozovatsky, I.D., E.G. Morozov, S.M. Shapovalov, A.V. Sokov, and S.A. Dobrolyubov, "Elements of transformation of Antarctic Intermediate Water and Antarctic Bottom Water north of the Equator", *"Interhemispheric Water Exchange in the Atlantic Ocean"* (Eds: Gustavo Goni and Paola Malanotte-Rizzoli), Elsevire, 2003 (under revision).

Navrotsky, V.V., I.D. Lozovatsky, E.P. Pavlova, and H.J.S. Fernando, "Observations of Internal Waves and Thermocline Splitting at the Shelf Break of the Japanese Sea", *Continental Shelf Res.*, 2002b (submitted)

Paka, V. T., V. N. Nabatov, I. D. Lozovatsky, and T. M. Dillon, "Oceanic microstructure measurements by "Baklan" and "Grif"," *J. Atmos. and Ocean Tech.*, 16(11), 1519-1532, 1999.

REFERENCES

Dillon, T. M., "Vertical overturns: A comparison of Thorpe and Ozmidov length scales", *J. Geophys. Res.*, **87**, 9601-9613, 1982.

Holloway, P.E. and M. Merrifield, "Internal tide generation by seamounts, ridges and islands", *J. Geophys. Res.*, **104**, 25937-25951, 1999.

Gibson, C. H., "Fossil temperature, salinity and vorticity turbulence in the ocean", *Marine Turbulence*, edited by J. C. J. Nihoul, 221-257, Elsevier, Amsterdam, 1980.

Gibson, C. H., V. N. Nabatov, and R. V. Ozmidov, "Measurements of turbulence and fossil turbulence near Ampere seamount", *Dyn. of Atmos. and Oceans,* **19**, 175-204, 1993.

Inall, M.E., T.P. Rippeth, and T.J. Sherwin, "Impact of nonlinear waves on the dissipation of internal tidal energy at a shelf break", *J. Geophys. Res.*, **105**, C4, 8687-8705. 2000.

Kunze, E. and J. Toole, "Tidally driven vorticity, diurnal shear, and turbulence atop Fieberling seamount", *J. Phys. Oceanogr.*, **27**, 2663-2693, 1997.

McComas, C.H., and P. Muller, "The dynamic balance of internal waves", *J. Phys. Oceanogr.*, **11**, 970-986, 1981.

Morozov, E.G., "Semidiurnal internal wave global field", *Deep-Sea Res.*, **42**, 135-148, 1995.

Morozov E.G., and V.I. Vlasenko, "Extreme tidal internal waves near the Mascarene Ridge", *J. Marine Sys.*, **9**(3-4), 203-210, 1996.

Navrotsky, V.V., "Mixing caused by internal waves and turbulence: A comparative analysis", *J. Marine Sys.*, **21**(1-4), 131–145, 1999.

Navrotsky V.V., V.L. Izergin, and E.P.Pavlova., "Internal wave generation near the shelf boundary", *Earth Sci., Doklady Rus. Acad. Sci.*, 2002a, (in press).

Phillips, O.M., "Turbulence in strongly stratified fluid - is it unstable?", *Deep-Sea Res.*, **19**, 79-81, 1972.

Posmentier, E.S., "The generation of salinity fine structure by vertical diffusion", *J. Phys. Oceanogr.*, **7**, 298-300, 1977.

Pringle, J.M., "Observations of high-frequency internal waves in the Coastal Ocean Dynamics Region", *J. Geophys. Res.*, **104**(C3), 5263-5281, 1999.